Interfacial behaviour of bovine testis hyaluronidase

Silvia Belem-Gonçalves, Pascale Tsan, Jean-Marc Lancelin, Tito L. M. Alves, Vera M. Salim, Françoise Besson, Françoise Besson

Biochemical Journal Immediate Publication. Published on 13 Jun 2006 as manuscript BJ20060485

Interfacial Behaviour of Bovine Testis Hyaluronidase

Silvia Belem-Gonçalves*,‡, Pascale Tsan†, Jean-Marc Lancelin†, Tito L. M. Alves‡, Vera M. Salim‡ and Françoise Besson*

*Laboratoire Organisation & Dynamique des Membranes Biologiques, UMR-CNRS 5013, Université Claude Bernard Lyon I, 43, boulevard du 11 novembre 1918, F-69622 Villeurbanne Cedex, France.

†Laboratoire de RMN Biomoléculaire, CNRS UMR 5180, Université Claude Bernard-Lyon 1, 43, boulevard du 11 novembre 1918, F-69622 Villeurbanne, France.

‡Programa de Engenharia Química/COPPE, Universidade Federal do Rio de Janeiro, Centro de Tecnologia, CP 68502, Rio de Janeiro, 21945-970, RJ, Brazil.

Corresponding author:

Françoise Besson, Laboratoire Organisation et Dynamique des Membranes Biologiques, UMR-CNRS 5013, Université Claude Bernard Lyon I, 43, boulevard du 11 novembre 1918, F-69622 Villeurbanne Cedex, France.

Phone: +33 04 72 44 83 24.

Fax: +33 04 72 43 15 43.

E-mail: f-besson@univ-lyon1.fr

Short title:

Interfacial Behaviour of Bovine Testis Hyaluronidase

Biochemical Journal Immediate Publication. Published on 13 Jun 2006 as manuscript BJ20060485

SYNOPSIS

The interfacial properties of bovine testicular hyaluronidase were suggested by demonstrating the association of hyaluronidase activity with membranes prepared from bovine testis. Protein adsorption to the air/water interface was investigated using surface pressure-area isotherms. Whatever the way to obtain interfacial films (protein injection or deposition), the hyaluronidase exhibited a significant affinity for the air/water interface. The isotherm obtained 180 min after protein injection into a pH 5.3 subphase was similar to the isotherm obtained after spreading the same amount of protein on the same subphase, indicating that bovine testicular hyaluronidase molecules adopted similar arrangement and/or conformation at the interface. Increasing the subphase pH from 5.3 to 8 resulted in changes of the protein isotherms. These modifications, which could correspond to the small pH-induced conformational changes observed by FTIR spectroscopy, were discussed in relation with the pH influence on the hyaluronidase activity. Adding hyaluronic acid, the enzyme substrate, to the subphase tested the stability of the hyaluronidase interfacial properties. The presence of hyaluronic acid in the subphase did not modify the protein adsorption and allowed the substrate binding to a preformed film of hyaluronidase at pH 5.3, the optimal pH for the enzyme activity. Such effects of hyaluronic acid were not observed when the subphase was constituted of pure water, medium where the enzyme activity was negligible. These influences of hyaluronic acid were discussed in relation with the modelled structure of bovine testis hyaluronidase where a hydrophobic region was supposed to be at the opposite of the catalytic site.

Key words

Bovine testis hyaluronidase, hyaluronic acid, Langmuir film, FTIR spectroscopy.

Abbreviations

FTIR, Fourier Transform Infrared; GPI, glycosylphosphatidylinositol; Ks, surface elasticity modulus.

Biochemical Journal Immediate Publication. Published on 13 Jun 2006 as manuscript BJ20060485

INTRODUCTION

Hyaluronidases are present in many tissues and organs (such as kidney, liver, skin, testes and uterus), as well as in venom (bees, wasps or cobra) [1]. These enzymes are capable of hydrolysing randomly hyaluronic acid [2], one of the most abundant constituents of the extracellular matrix [3-4]. They also act on chondroitin or chondroitin sulphates [5-8]. Hyaluronidases are implicated in many biological functions, including allergy [9], inflammation [10-13], migration of cancer cells [14] and microvascular permeability [15].

Six human hyaluronidases have been to date cloned [16], and three of them have been expressed in different cell lines, but, due to difficult isolation and/or purification, the enzymes have not been produced in enough amounts for enzymatic characterisation and structural determination. Moreover bovine testicular hyaluronidase, which is commercially avaible, has been chosen as a model for several studies. Thus, the hyaluronan hydrolysis catalysed by this enzyme has been studied by investigating the hydrolysis kinetics at pH 5 and 37 °C [17]. The authors demonstrated that the hyaluronan hydrolysis by hyaluronidase was inhibited at high substrate concentration and low ionic strength and suggested the formation of non-specific complexes between hyaluronan and hyaluronidase based on electrostatic interactions. Furthermore Monte Carlo simulation of the mechanism of bovine testicular hyaluronidase reaction showed that condensation reaction is much weaker than the transglycosylation reaction but contributes to product distribution at the final stage of the reaction, preventing complete hydrolysis of the substrates [18].

Even if bovine testicular hyaluronidase and the distantly related bee venom hyaluronidase are well known representatives of the eukaryotic enzymes, structural information is only available for the bee venom hyaluronidase [19]. This is the reason why we were interested in the characterisation of bovine testicular hyaluronidase. In this work, we looked for interfacial properties of the bovine testicular hyaluronidase because we demonstrated that, in a bovine testis homogenate, a significant amount of the hyaluronidase activity could be recovered associated with membranes. We then modelled the bovine testicular hyaluronidase by using crystal structure of the bee venom hyaluronidase in order to localize the hydrophobic amino acids on the surface of the molecule. Thus the suspected interfacial properties of the protein were studied by using the commercial bovine testicular hyaluronidase and the ability of this protein to

form films at the air-water interface in different conditions were investigated. The pH-sensitive interfacial properties of the enzyme were compared with the pH-sensitive enzymatic activity of the protein on hyaluronic acid as well as with the pH-induced conformational changes evidenced by FTIR spectroscopy. Finally the influence of hyaluronic acid on the interfacial properties of the bovine testicular hyaluronidase was studied.

MATERIALS and METHODS

Materials

Hyaluronic acid from human umbilical cord and hyaluronidase from bovine testis (type IV-S) were purchased from Sigma-Aldrich and deuterated water (^2H_2O) from Merck. All organic solvents were analytical grade.

Isolation of bovine testis membranes

Total membranes were prepared as previously described for bovine kidney [20] with minor modifications. Bovine testis tissue was cut into small pieces and homogenized in 10 mM Tris buffer, pH 7.4 containing 150 mM NaCl (Tris buffer) and 0.25 M sucrose with pepstatin and leupeptin (0.25 mM each). The homogenate was centrifuged at 150,000 g for 30 min at 4°C. The pellets containing total membranes were further washed three times at 4°C with the same buffer and centrifuged at 150,000 g as above.

Protein and enzyme assays

Protein concentrations were determined by the method of Bradford [21] using bovine serum albumin as standard. Hyaluronidase activity was measured in a 100 mM phosphate buffer pH 5.3 containing 150 mM NaCl as previously described [22]. One enzyme unit hydrolyzes half of the hyaluronic acid present in the assay during the 10 min reaction time. Alkaline phosphatase activity was measured at 37°C in a 25 mM glycine buffer pH 11 containing p-nitrophenyl phosphate as substrate. Release of p-nitrophenolate was followed at 420 nm. One enzyme unit hydrolyzes one µmole p-nitrophenyl phosphate /min [20].

Monolayer technique

All experiments were performed at a constant temperature of 21.0 ± 0.1 °C. The film balance was built by R&K (Riegler & Kirstein, Wiesbaden, Germany) and equipped with a Wilhelmy-type surface-pressure measuring system as previously described [23]. The subphase buffer used was a 100 mM phosphate buffer containing or not 150 mM NaCl at different pH. In all experiments, the subphase was continuously stirred with a magnetic stirrer spinning at 100 rpm. In order to measure the hyaluronidase adsorption at constant surface area, the experiments were performed on a small Teflon dish (diameter, 3 cm) with a subphase volume of 7 mL. The enzyme was injected in the subphase at a final concentration of 1.4 µg/mL. Hyaluronidase adsorption at the air-water interface, measured by tensiometry, was followed as an increase in surface pressure. The π-A isotherms of the protein were measured either after deposition or after injection of a known quantity of hyaluronidase either on or into the subphase buffer of the Langmuir trough (dimensions: 165 cm² and 120 mL subphase). After 15 min, the surface was compressed at a velocity of 6 cm²/min. The adsorption times indicated on the compression-decompression-recompression π-A isotherms correspond to the cumulated adsorption time at zero surface pressure. Indeed, we consider that the protein is weakly adsorbed at the interface during the decompression.

Surface elasticity moduli were calculated from the pressure-area data obtained from the monolayer compressions using the following equation: $Ks = -Ad\pi/dA$, where A is the molecular area at the indicated surface pressure π.

FTIR spectroscopy measurements

Infrared data were acquired, as previously described [24], with a Nicolet 510M FTIR spectrometer continuously purged with dry filtered air (Balston regenerating desiccant dryer). Spectra were recorded at 25°C with 128 interferograms and Fourier transformed. The resolution was 4 cm^{-1}. 20 µl of a hyaluronidase solution at 10 mg/mL, freshly prepared in a 100 mM phosphate ^2H_2O buffer containing 150 mM NaCl at different pH, were deposited into a CaF_2 cell. The final spectrum was fitted by the mean of a curve fitting program computing the Lorentzian band shape components in the amide I region. The wavenumber position of each component band was fixed while the width and the height varied in order to obtain the best fit. The wavenumber position and the number

of component bands were determined by using the second derivative spectra. After decomposition, the percentage of each component band was calculated as 100 (Ax/At), where Ax is a component band area and At is the amide band area. IR difference spectra were obtained by using the intensity of the characteristic Tyr band at 1515 cm^{-1} as reference for the hyaluronidase concentration.

Modelling of the three-dimensional structure of bovine testicular hyaluronidase

Bovine testicular hyaluronidase (sequence accession code Q7YS45; [25]) were modelled with version 4.0 of the MODELLER program [26] using the hyaluronidase from bee venom, the closest three-dimensional structure available (1FCU Protein Data Bank accession code; [19]) and the sequence alignment shown in Fig. 1.

RESULTS

Hyaluronidase from bovine testis is membrane-bound

During assays for preparation of hyaluronidase from bovine testis, an unexpected result was obtained. Indeed a testicular homogenate was prepared and separated by classical centrifugation at 150,000 g to obtain a soluble protein supernatant and a total membrane pellet. Only about 50% of the hyaluronidase activity of the homogenate were recovered in the soluble protein fraction. To test the efficiency of the membrane preparation, the activity of alkaline phosphatase, a GPI-anchored membrane marker [20], was titrated in parallel with the activity of hyaluronidase. About 80% of the alkaline phosphatase activity of the homogenate were recovered associated with membranes, showing a good separation of the membranes. Furthermore three washings of total membranes with buffer did not induce a release of both enzymes. Since it had been demonstrated that the bovine testicular hyaluronidase does not possess a lipidic modification [27], its membrane association could be due to amphiphilic properties.

Hyaluronidase modelling

We then looked for the repartition of hydrophobic amino acids (potent candidates to induce amphiphilic properties of proteins) on the surface of the bovine testicular hyaluronidase molecule after constructing the 3D model of this enzyme on the base of the known crystal structure of bee venom hyaluronidase [19]. The sequence alignment used is given in Fig. 1 showing that there are an N-terminal region (corresponding to 12

amino acids) and a C-terminal region (corresponding to about 100 amino acids) which were not be modelled. Fig. 1 also shows the presence of several groups of hydrophobic amino acids along the sequence and Fig. 2 indicates the repartition of the hydrophobic amino acid residues on the surface of the modelled molecule of testicular hyaluronidase. The top view shows the presence of a hydrophobic patch around the N- and C-terminal regions of the testicular enzyme and the lateral view shows that this hydrophobic regions are located more or less at the opposite of the catalytic site containing two conserved negatively charged amino acids.

Hyaluronidase adsorption at the air-water interface

The hyaluronidase amphiphilic properties suggested by its membrane association and its modelling led us to investigate possible interfacial properties of the protein. This was first studied by determining the adsorption of protein at the air-water interface. The same amount of protein (12 µg) was injected into different pH subphases, giving a final enzyme concentration of 1.4 µg/mL. The adsorption was monitored by measuring the surface pressure at constant area as a function of time. When injected into the subphase at pH 5.3 (Fig. 3), a lag time of about 20 min was necessary to detect the protein at the interface. Then the surface pressure increased gradually until a maximum was reached after about 70 min, indicating that a stable monolayer was formed at the interface. Varying the pH subphase did not significantly modify the kinetic of the protein adsorption (Fig. 3).

If our data are compared with the air-water interface adsorption of the amyloid precursor protein (APP), which has been shown to exhibit interfacial properties [28], it appears that, at similar concentrations, hyaluronidase and APP show similar adsorption kinetic. This indicates that hyaluronidase effectively exhibits interfacial properties.

Hyaluronidase isotherms

Then the adsorption of the protein at the air-water interface was followed by measuring successive π-A isotherms after injection of 12 µg of hyaluronidase into the trough subphase buffer to reach a final concentration of 0.1 µg/mL. The trough surface was compressed after various delays to obtain π-A isotherms presented in Fig. 4A. The molecular area at each surface pressure increased with increasing time, indicating that the protein was adsorbed at the air-water interface [29-30]. The protein adsorption was

not measured over 180 min since the isotherm obtained after that time was similar to that obtained when the 12 µg of protein was deposited onto the subphase buffer, indicating that, after a 180 min delay, roughly all the protein had reached the interface (Fig. 4A).

The surface elasticity modulus (Ks) of the last π-A isotherm was represented against the surface pressure in Fig. 4B. The variation of Ks during the compression exhibits three phases. During the first phase, the Ks increased linearly until the surface pressure reached 5 mN/m. For pressures between 8 and 12 mN/m, the Ks increase was lower and stabilised and for pressure higher than12 mN/m the Ks decreased.

Influence of the buffer composition on the hyaluronidase isotherm

We were then interested in the influence of pH on the interfacial properties of the hyaluronidase. The protein was dissolved in the corresponding subphase buffer and spread at the air-water interface. Measuring π-A isotherms were after spreading the protein on different buffered subphases tested the influence of pH on the interfacial properties of hyaluronidase (Fig. 5). The hyaluronidase isotherms were shifted to lower molecular area at pH 5.3 and pH 6.2 as compared with pH 7.2 and pH 8. These shifts decreased during the compression of the hyaluronidase monolayer and at the highest pressures, all the curves tend to the same value. Similar experiments were performed with hyaluronidase solubilized in water with a water subphase (Fig. 5). In these conditions the shift toward higher molecular area is observed all along the isotherm.

Influence of hyaluronic acid on the hyaluronidase adsorption

The absence of interfacial properties of hyaluronic acid was first tested. Hyaluronic acid was injected at 8.3 µg/mL into pH 5.3 buffer or water subphases. Thirty minutes after the injection and at several 30-min intervals, the interface was compressed and the pressure was measured during the compression. No variation of the pressure was observed whatever the subphase or the waiting time, indicating the absence of interfacial property for the hyaluronidase substrate.

The influence of hyaluronic acid on the protein ability to reach the air-water interface was then tested. Successive π-A isotherms were measured after injecting 0.1 µg/mL hyaluronidase into pH 5.3 buffer subphase containing 3.3 µg/mL hyaluronic acid and were compared with those obtained in the absence of enzyme substrate. For each

adsorption delay, isotherms obtained with or without hyaluronic acid were pratically superposed. Increasing hyaluronidase concentration up to 0.2 µg/mL allowed the detection of small differences in the adsorption kinetics as seen in (Fig. 6).

Similar experiments were performed with hyaluronidase solubilized in water and injected at 0.2 µg/mL in a water subphase containing, or not, 3.3 µg/mL hyaluronic acid. Successive π-A isotherms were measured during the protein adsorption and the pressures induced by the protein adsorption at an area of 20 cm² were plotted versus the adsorption delays (Fig. 6). In the absence of hyaluronic acid, the protein in water subphase reached the interface more slowly than it did at the same concentration in pH 5.3 subphase. In the presence of hyaluronic acid, the protein in water induced no significant pressure during interface compression, indicating that the protein remained in the subphase.

Adsorption of hyaluronic acid on the hyaluronidase monolayer

We then tested if the interaction between the enzyme and its soluble substrate would destabilise hyaluronidase films at the air-water interface. So the hyaluronidase was spread at the surface of the pH 5.3 buffer subphase containing different concentrations of hyaluronic acid (1.7 or 3.3 µg/mL) and the isotherms were measured 30 min after the protein deposition. For the two hyaluronic acid concentrations, the isotherms measured in the presence of hyaluronic acid were compared to the isotherm measured in its absence (Fig. 7A). In all the cases, the isotherms measured with hyaluronic acid shifted toward higher molecular area as compared with the isotherm without hyaluronic acid. These shifts increased with increasing the hyaluronic acid concentration. Furthermore, when the isotherms were measured 60 min after the injection of hyaluronic acid no significant changes were observed as compared with the isotherms obtained 30 min after the injection (data not shown). The surface elasticity moduli (Ks) of the π-A isotherm before and after hyaluronic acid injection were represented against the surface pressure in Fig. 7B. For the lowest surface pressures (until about 7 mN/m), Ks were increased in the presence, confirming that the interaction between the hyaluronidase and its substrate.

The influence of the subphase on the interaction between hyaluronic acid and hyaluronidase was then tested. When the pH of the buffer subphase was increased from 5.3 to 8 and the protein was dissolved in the corresponding buffer, the isotherm shifts

toward higher molecular area were still observed in the presence of hyaluronic acid (data not shown). On the contrary, such a shift of the isotherm toward higher molecular area was not observed when the protein dissolved in water was spread on a water subphase (Fig. 7A).

FTIR spectroscopy studies of the secondary structure of hyaluronidase

The differences observed in the interfacial properties of the enzyme with the wide variations of pH, as well as interaction with hyaluronic acid, may influence the conformation of the bovine hyaluronidase. Indeed some amino acid residues may change their local charges and potentially flexible hydrophobic segments buried in the molecule may move to the surface of molecule during its movement to the interface. This is the reason why FTIR spectroscopy was used to look for pH-induced changes in the conformation of hyaluronidase.

The ^2H_2O buffer-subtracted FTIR spectrum of hyaluronidase at pH 5.3 (p^{2}H 5.5) and its deconvolution are shown in Fig. 8. Amide I bands, at 1700-1610 cm^{-1}, are principally C=O stretching vibrations with some N-H bending and C-H stretching vibrations while amide II bands, at 1575-1480 cm^{-1}, are principally N-H bending vibrations with some CN stretching vibrations. The remaining intense amide II component band at 1545 cm^{-1} pointed out an incomplete NH/N^{2}H exchange. This incomplete deuteration corresponds to N-H residues buried in the hydrophobic regions of the protein since increasing the incubation time in the ^2H_2O buffer did not modify the amide II band intensity. The deconvolution of the amide I bande gives four component bands at 1634, 1650, 1657 and 1675 cm^{-1}. The 1634 cm^{-1} band associated with the 1675 cm^{-1} band corresponds to intramolecular β-sheets, although overlap from β-turns can also contribute to this last band. The 1657 cm^{-1} band in ^2H_2O is usually produced by α-helices but it cannot be excluded to originate from turns or 3_{10}-helices. The 1650 cm^{-1} band in ^2H_2O corresponds to unordered structures. Besides, it is well known that some amino acid side chain groups absorb in amide I and II regions [31]. The 1515 cm^{-1} band, corresponding to Tyr residues, was easily recognized while the bands at 1585 and 1565 cm^{-1} might correspond to Asp and Glu COO^- residues. The four amide I component bands at 1675, 1657, 1650 and 1634 cm^{-1}, represent respectively 6, 20, 33 and 41% of the original band.

Then, in order to explain the pH-sensitivity of the hyaluronidase, we looked for hypothetical pH-induced conformational changes of this protein. ^2H_2O buffer-subtracted FTIR spectra of hyaluronidase with increasing pH show a slight decrease in the maximum of the amide I band (from 1643 cm^{-1} at pH 5.3, to 1642 cm^{-1} at pH 6.2, 1641 cm^{-1} at pH 7.2 and 1640 cm^{-1} at pH 8) and a decrease in intensity of the amide II band, pointing out a NH/N²H exchange increase (Fig. 9A). The pH-induced conformational changes of hyaluronidase could be better seen on the IR difference spectra, obtained by subtracting the FTIR spectrum of hyaluronidase at pH 5.3 to the FTIR spectrum at another pH (Fig. 9B). When pH varied from 6.2 to 8, the negative bands of the IR difference spectra at 1657 cm^{-1}, corresponding to α-helices, decreased in intensity while the positive bands at 1625 cm^{-1}, corresponding to intermolecular β-sheets, increased. This indicates that intermolecular β-sheets appeared at the expense of α-helices. At pH 8, the positive peak of the IR difference spectrum at 1625 cm^{-1} involved 2-3 % of the amino acids of the protein, meaning that about 11 amino acids were implicated in the formation of intermolecular β-sheets. Furthermore the FTIR spectrum of hyaluronidase measured in non-buffered ^2H_2O was compared with the spectrum measured at pH 5.3 and the resulting IR difference spectrum was similar to that obtained by subtracting the FTIR spectrum at pH 5.3 to the FTIR spectrum at pH 6.2 (data not shown).

DISCUSSION

Sperm and testicular hyaluronidases have the same amino acid sequence but differ by their post-translational modification [27]. Indeed the sperm hyaluronidase possesses a GPI anchor while the testicular hyaluronidase does not. In this work, we showed that the total membranes, obtained by classical centrifugation at 150,000 g of a bovine testis homogenate, contained hyaluronidase and that three washings of total membranes with buffer did not induce a release of the enzyme. This unexpected membrane association could be explained if bovine testicular hyaluronidase possesses amphiphilic properties. In order to test this hypothesis, the presence of surface hydrophobic areas at the surface of the bovine testicular hyaluronidase molecule was estimated after modelling the protein with the crystal structure of the bee hyaluronidase. A hydrophobic region, more or less at the opposite of the catalytic site, was evidenced at the surface of the bovine testicular hyaluronidase molecule. This region could be responsible for the amphiphilic properties of the protein but it must be remembered that the modelling did not involved

all the amino acids of the protein. Indeed the non-modelled C-terminal peptide part, which is not significantly enriched in hydrophobic amino acids, could mask the hydrophobic region.

One of the factors contributing to the affinity of the protein for the interface is the presence of hydrophobic areas on the surface of the protein [32]. The monolayer technique, which is a powerful method for assaying the surface activities of proteins [33], was then applied to bovine testicular hyaluronidase. Another important advantage of this method is that its requires only small amounts of proteins. Following the protein adsorption by direct measure of the pressure increase after injection into a small trough shows that bovine testicular hyaluronidase exhibits a significant surface activity. Measuring successive isotherms after protein injection was the other way chosen to determine the enzyme adsorption at the air/buffer interface in a time-dependent manner. Furthermore, it was shown that hyaluronidase remains at the interface when spread and the surface pressure developed by the protein after injection, as a consequence of its adsorption at the interface, leads to values similar to those obtained by direct spreading onto the surface. This indicates that, as it has been shown for other proteins [33-36], the arrangement adopted by the bovine testicular hyaluronidase at the interface is independent of the method used to form the film. This was confirmed by the similarities in the pressure-dependent variations of surface elasticity modulus (Ks) observed after injection or spreading. Furthermore, the Ks variations suggest that compression induce a marked rearrangement of the organisation and distribution of the protein at the interface. One may consider that the plateau, observed between 8 and 12 mN/m, could be due to equilibrium between the protein desorption and adsorption at the air-water interface. It seems that above 12 mN/m, there was either a protein desorption or a reorganisation of the protein at the air-water interface during the monolayer compression. It is interesting to notice that the maximum value of the surface elasticity modulus (at about 30 mN/m) was obtained at a pressure (10 mN/m) similar to those observed for the phospholipid-hydroperoxide glutathione peroxidase [37] and for the creatine kinase [34].

Several factors (pH, salts and hyaluronic acid concentration as well as the glycosaminoglycan microenvironment of hyaluronidase) are known to affect the enzymatic activity of bovine testicular hyaluronidase [5, 17, 38]. Increasing the subphase pH from 5.3 to 8 (corresponding to a decrease of the optimal conditions for

the enzymatic activity of hyaluronidase) induces small but significant differences in the π-A isotherms. This might reflect pH-induced differences either in the desorption of protein segments or in the short-range intermolecular interactions. Indeed decreasing the pH could decrease the repulsive forces between the protein molecules by neutralising some ionic charges on the protein surface since the pI of the bovine testicular hyaluronidase is about 5 [39]. Similarly, the larger shift observed in the isotherm measured on water (condition which gives only 7% of the enzymatic activity measured at pH 5.3) could be explained by the absence of salts. Furthermore the variations observed in the isotherms could result from the small structural changes observed by FTIR spectroscopy.

Since hydrophobic interactions on the surface of the hyaluronidase molecule have been previously suggested to play a role during the formation of conjugates between hyaluronidase and glycosaminoglycans [40], we then looked for the surface activity of the protein in the presence of its substrate, the hyaluronic acid. In a first set of experiments, the influence of hyaluronic acid on the hyaluronidase ability to reach the interface was followed by measuring successive π-A isotherms after injection of the protein into a pH 5.3 buffered subphase containing, or not, the enzyme substrate. In these conditions (corresponding to the optimal conditions for the enzymatic activity), hyaluronic acid did not significantly decrease the amount of hyaluronidase detected at the interface. The presence of the catalytic site at the opposite of the hydrophobic region (as suggested by protein modelling) could explain the persistence of the adsorption of the protein in the presence of hyaluronic acid.

In a second set of experiments, injecting the enzyme substrate under a pre-formed film of hyaluronidase on a pH 5.3-buffered subphase followed the influence of hyaluronic acid on the hyaluronidase ability to remain at the air-water interface. Whatever the substrate concentration, the isotherms measured in the presence of hyaluronic acid shifted toward higher molecular area as compared with the isotherm in its absence. These shifts increased with increasing the hyaluronic acid concentration. This indicates that the presence of the water-soluble hyaluronic acid into the subphase did not induce a delocalisation of the protein from the air-water interface to the bulk subphase (no shift of the isotherm toward lower molecular area). Furthermore, the isotherm shift toward higher molecular area showed that the protein at the interface was still able to interact with the hyaluronic acid, the complex "hyaluronidase-hyaluronic acid" having a higher

molecular area than the protein alone. Moreover, the absence of significant changes between the isotherms measured at different times after the hyaluronic acid injection might suggest that the enzyme binding to its substrate occurred faster than the hyaluronic acid hydrolysis by hyaluronidase. The experiment temperature (21°C) which is lower than the physiological temperature could explain this result.

Moreover, the subphase influences the interaction between hyaluronidase and its substrate. When the pH of the buffer subphase varied from 5.3 to 8 (pH range allowing the hydrolysis of hyaluronic acid by the enzyme, even if there is a decrease of enzymatic activity), the presence of hyaluronic acid induces isotherm shifts toward higher molecular area. On the contrary, when the subphase contained only water (condition which did not induce significant hyaluronic acid hydrolysis), such a shift toward higher molecular area was not observed. Furthermore, when hyaluronidase was injected into a water subphase, it reached the interface more slowly than the protein injected into the subphase at pH 5.3, the pI of the protein, and the addition of hyaluronic acid induced the remaining of the protein into the subphase. The hyaluronic acid-induced inhibition of the adsorption of the protein in water could be due either to an increase of the charges at the surface of the molecule or to a partial denaturation of the hyaluronidase, masking the hydrophobic region of the protein.

In conclusion we have shown that bovine testicular hyaluronidase exhibits surface activity depending on the composition of the medium where it was solubilized. Maximum of interfacial properties was observed in conditions corresponding to the maximum of enzymatic activity. At this stage, a deeper knownledge of the influence of the pH as well as a better characterization of the interactions between the protein and hyaluronic acid at the air-water interface, which might influence the 3D structure of the bovine hyaluronidase are necessary. Such studies would need the use of specific interfacial biophysical techniques.

ACKNOWLEDGEMENTS

S. B. G. was recipient of a Ph.D. fellowship from the Brazilian government (CAPES, Project N° BEX 0801/04-6). We thank A. Kouzayha for helpful discussions.

REFERENCES

1. Kreil, G. (1995) Hyaluronidases - a group of neglected enzymes. Protein Sci. **9**, 1666-1669

2. Tranchepain, F., Deschrevel, B., Courel, M. N., Levasseur, N., Le Cerf, D., Loutelier-Bourhis, C. and Vincent, J. C. (2006) A complete set of hyaluronan fragments obtained from hydrolysis catalyzed by hyaluronidase: Application to studies of hyaluronan mass distribution by simple HPLC devices. Anal. Biochem. **348**, 232-242

3. Toole, B. P. (2004) Hyaluronan: from extracellular glue to pericellular cue. Nat. Rev. Cancer **7**, 528-539

4. Laurent, T.C. and Fraser, J. R. E. (1992) Hyaluronan. FASEB J. **6**, 2397-2404

5. Csoka, T. B., Frost, G. I. and Stern, R. (1997) Hyaluronidases in tissue invasion. Invasion Metastasis **17**, 297-311

6. Saitoh, H., Takagaki, K., Majima, M., Nakamura, T., Matsuki, A., Kasai, M., Narita, H. and Endo, M. J. (1995) Enzymatic reconstruction of glycosaminoglycan oligosaccharide chains using the transglycosylation reaction of bovine testicular hyaluronidase. J. Biol. Chem. **270**, 3741-3747

7. Takagaki, K., Munakata, H., Majima, M. and Endo, M. (1999) Enzymatic reconstruction of a hybrid glycosaminoglycan containing 6-sulfated, 4-sulfated, and unsulfated N- acetylgalactosamine. Biochem. Biophys. Res. Commun. **258**, 741-744

8. Takagaki, K., Munakata, H., Kakizaki, I., Majima, M. and Endo, M. (2000) Enzymatic reconstruction of dermatan sulfate. Biochem. Biophys. Res. Commun. **270**, 588-593

9. Kakegawa, H., Matsumoto, H. and Satoh T. (1988) Inhibitory effects of hydrangenol derivatives on the activation of hyaluronidase and their antiallergic activities. Planta Medica **54**, 385-389

10. Szary, A., Kowalczyk-Bronisz, S. H. and Gieldanowski, J. (1975) Indomethacin as inhibitor of hyaluronidase. Arch. Immunol. Ther. Exp. Warsz. **23**, 131-134

11. Feinberg, R. N. and Beebe, D. C. (1983) Hyaluronate in vasculogenesis. Science **220**, 1177-1179

12. West, D. C. and Kumar S. (1989) The effect of hyaluronate and its oligosaccharides on endothelial cell proliferation and monolayer integrity. Exp. Cell Res., **183**, 179-196

13. Horton, M. R., Mckee, C. M., Bao, C., Liao, F., Farber, J. M., Hodge-Du-Four, J., Purae, E., Oliver, B. L., Wright, T. M. and Noble, P. W. (1998) Hyaluronan fragments

synergize with interferon-gamma to induce the C-X-C chemokines mig and interferon-inducible protein-10 in mouse macrophages. J. Biol. Chem. **273**, 35088-35094

14. Cameron, E., Pauling, L. and Leibovitz, B. (1979) Ascorbic acid and cancer: a review. Cancer Res. **39**, 663-681.

15. Sunnergren, K.P. and Rovetto, M.J. (1985) The effects of hyaluronidase on interstitial hydration, plasma protein exclusion, and microvascular permeability in the isolated perfused rat heart. Microvasc Res. **30**, 286-297.

16. Csoka, A. B., Frost, G. I. and Stern, R. (2001) The six hyaluronidase-like genes in the human and mouse genomes. Matrix Biol. **20**, 499-508

17. Asteriou, T., Vincent, J. C., Tranchepain, F. and Deschrevel, B. Inhibition of hyaluronan hydrolysis catalysed by hyaluronidase at high substrate concentration and low ionic strength. Matrix Biol. In press

18. Nakatani, H. (2002) Monte Carlo simulation of hyaluronidase reaction involving hydrolysis, transglycosylation and condensation. Biochem. J. **365**, 701-705.

19. Markovic-Housley, Z., Miglinerini, G., Soldatova, L., Rizkallah, P., Müller, U., and Schirmer, T. (2000) Crystal structure of hyaluronidase, a major allergen of bee venom. Structure (Lond.) **8**, 1025-1035

20. Bonnin, S., El Kirat, K., Becchi, M., Dubois, M., Grangeasse, C., Giraud, C., Prigent, A-F., Lagarde, M., Roux, B. and Besson, F. (2003) Protein and lipid analysis of detergent-resistant membranes isolated from bovine kidney. Biochimie **85**, 1237-1244

21. Bradford, M. M. (1976) A rapid and sensitive method for quantitation of microgram quantities of protein utilizing the principle of protein-dye binding. Anal. Biochem. **72**, 248-254

22. Borders, C. L. Jr and Raftery, M. A. (1968) Purification and partial characterization of testicular hyaluronidase. J. Biol. Chem. **243**, 3756-3762

23. El Kirat, K., Besson, F., Prigent, A-F., Chauvet, J-P. and Roux, B. (2002) Role of calcium and membrane organization on phospholipase D localization and activity. Competition between a soluble substrate and an insoluble substrate. J. Biol. Chem. **277**, 21231-21236

24. Bonnin, S., Besson, F., Gelhausen, M., Chierici, S. and Roux, B. (1999) A FTIR spectroscopy evidence of the interactions between wheat germ agglutinin and *N*-acetyl-glucosamine residues. FEBS Lett. **456**, 361-364

25. Chowpongpang, S., Shin, H. S. and Kim, E. K. (2004) Cloning and characterization of the bovine testicular PH-20 hyaluronidase. Biotechnol. Lett. **26**, 1247-1252

26. Sali, A. & Blundell T. L. (1993) Comparative protein modelling by satisfaction of spatial restraints. J. Mol. Biol. 234, 779-815

27. Meyer, M. F, Kreil, G. and Aschauer, H. (1997) The soluble hyaluronidase from bull testes is a fragment of the membrane-bound PH-20 enzyme. FEBS Lett. **413**, 385-388

28. Lahdo, R., Coillet-Matillon, S., Chauvet, J. P. and de La Fournière-Bessueille, L. (2002) The amyloid precursor protein interacts with neutral lipids. Eur. J. Biochem. **269**, 2238-2246

1. Sanchez-Gonzalez, J., Cabrerizo-Vilchez, M. A. and Galvez-Ruiz, M. J. (2001) Interactions, desorption and mixing thermodynamics in mixed monolayers of β-lactoglobulin and bovine serum albumin. Colloids Surf. B: Biointerfaces **21**, 19-27

30. Gicquaud, C., Chauvet, J-P., Grenier, G., Tancrede, P. and Coulombe, G. (2003) Adsorption of actin at the air-water interface: a monolayer study. Biopolymers. **70**, 289-296

31. Barth, A. (2000) The infrared absorption of amino acid side chains. Prog. Biophys. Mol. Biol. **74**, 141-173

32. Wierenga, P., Meinders, M. B., Egmond, M. R., Voragen, F. A. G. and de Jongh, H. J. (2003) Protein exposed hydrophobicity reduces the kinetic barrier for adsorption of ovalbumin to the air-water interface. Langmuir **19**, 8964-8970

33. Graham, D. E. and Phillips, M. C. (1979) Proteins at liquid interfaces. J. Coll. Interface Sci. **70**, 404-439

34. Vernoux, N., Granjon, T., Marcillat, O., Besson, F. and Vial, C. Interfacial behaviour of cytoplasmic and mitochondrial creatine kinase oligomeric states. Biopolymers (2006) **81**, 270-281

35. Angeletti, S., Maggio, B. and Genti-Raimondi, S. (2004) Surface activity and interaction of StarD7 with phospholipid monolayers. Biochem. Biophys. Res. Commun. **314**, 181-185

36. Carrizo, M. E., Miozzo, M. C., Maggio, B. and Curtino, J. A. (2001) The amphiphilic character of glycogenin. FEBS Lett. **509**, 323-326

37. Morandat, S., Bortolato, M., Nicol, F., Arthur, J. R., Chauvet, J. P. and Roux, B. (2004) Adsorption of a phospholipid-hydroperoxide glutathione peroxidase into

phospholipid monolayers at the air-water interface. Colloids Surf. B Biointerfaces. **35**, 99-105

38. Maksimenko, A. V., Schechilina, Y. V., Tischenko, E.G. (2001) Resistance of dextran-modified hyaluronidase to inhibition by heparin. Biochemistry (Moscow) **66**, 456-463

39. Malmgren, H. (1953) Characteristics of testicular hyaluronidase. Biochem. Biophys. Acta. **4**, 524-529

40. Maksimenko, A.V., Schechilina, Y. V., Tischenko, E.G. (2003) Role of the glycosaminoglycan microenvironment of hyaluronidase in regulation of its endoglycosidase activity. Biochemistry (Moscow), **68**, 862-868

FIGURE LEGENDS

Figure 1. Sequence alignment of bovine testis hyaluronidase with bee venom hyaluronidase used for the modelling.

HYA_BOVINE refers to bovine testis hyaluronidase (sequence accession code Q7YS45) and HYA_BEE to bee venom hyaluronidase (Q08169). Regions in black boxes correspond to undefined structure in bovine hyaluronidase model (this work) or bee hyaluronidase crystal structure (1FCU Protein Data Bank accession code). Conserved residues of the active site (D112 and E114 in HYA_BOVINE, corresponding to D111 and E113 in HYA_BEE) are shown with bold letters. Hydrophobic amino acids of HYA_BOVINE, identified according to [http://www.inrp.fr/Acces/Biogeo/model3d/chimdata/scripts/globine/aa.htm], are underlined.

Figure 2. Hydrophobic residues in the model of bovine testis hyaluronidase (A, B).

A: Top view of the N- and C-terminal regions indicating C_{ter}, N_{ter} and hydrophobic amino acids (black area). B: View showing the N-terminal region opposite to the Asp and Glu conserved residues of the active site, as well as hydrophobic amino acids (black area). This modelled structure of bovine testis hyaluronidase did not take account of the amino acids in black boxes for HYA_BOVINE in Fig. 1.

Figure 3. Kinetics of surface pressure increases due to hyaluronidase adsorption at the air-water interface at 21°C.

12 µg-protein injections into a 100 mM phosphatase buffer containing 150 mM NaCl at pH 5.3 (open circles), pH 6.2 (full squares) and pH 7.2 (full diamonds).

Figure 4. Successive π-A isotherms during hyaluronidase adsorption at the air-water interface at 21 °C.

A: π-A isotherms measured 15 min (curve a), 35 min (curve b), 65 min (curve c), 125 min (curve d), and 180 min (curve e) after 12 µg-protein injection into pH 5.3 buffer subphase at zero surface pressure or after 12 µg-protein spreading (curve f). B: Monolayer Ks calculated from curve e isotherm and represented as a function of surface pressure.

Figure 5. Influence of pH on the hyaluronidase isotherms after 12 µg-protein spreading onto different buffer subphases at 21 °C.

Subphases were 100 mM phosphate, 150 mM NaCl buffer at pH 5.3 (full squares), pH 6.2 (open triangles), pH 7.2 (full circles), pH 8 (open diamonds) and pH 5.6 water (full triangles).

Figure 6. Kinetic of hyaluronidase adsorption at 21 °C.

The pressures induced by the protein adsorption (0.2 µg/mL) at a 20 cm² area (obtained from the π-A isotherms) were plotted versus the adsorption delays. Assays with pH 5.3 buffer (triangles) or pH 5.6 water (circles) subphases containing no (full lines) or 3.3 µg/mL (dotted lines) hyaluronic acid.

Figure 7. Influence of hyaluronic acid on preformed hyaluronidase films at 21 °C.

A: π-A isotherms of hyaluronidase dissolved in pH 5.3 buffer (full symbols) or in pH 5.6 water (open symbols) and spread onto pH 5.3 buffer or water subphases containing no hyaluronic acid (squares), 1.7 µg/mL (diamonds) or 3.3 µg/mL (triangles) hyaluronic acid. Isotherms were measured 30 min after the protein deposition. B: π-A isotherm-derived Ks of hyaluronidase in pH 5.3 buffer subphases containing no (curve a) or 1.7 µg/mL (curve b) hyaluronic acid.

Figure 8. $^{2}H_2O$ buffer-subtracted FTIR spectrum of hyaluronidase at pH 5.3.

Original spectrum (full line), best-fitted individual component bands of the amide I and II regions (full lines) and their resulting summation (dotted line). Protein concentration was 10 mg/mL.

Figure 9. Influence of pH on the FTIR spectra of hyaluronidase.
A: $^{2}H_2O$ buffer-FTIR spectra of hyaluronidase at pH 5.3 spectrum (a), 6.2 (b), 7.2 (c) and 8.0 (d). B: IR difference spectra obtained by subtracting the FTIR spectrum at pH 5.3 to FTIR spectra of hyaluronidase at pH 6.2 (a), 7.2 (b) and 8.0 (c).

Biochemical Journal Immediate Publication. Published on 13 Jun 2006 as manuscript BJ20060485

```
HYA_BOVINE      LDFRAPPLISNTSFLWAWNAPVERCVNRRFQLPPDLRLFSVKGSPQKSAT 50
HYA_BEE         ---TPDNNKTVREFNVYWNVPTFMCHKYGLRFEEVSEKYGILQNWMDKFR 47

HYA_BOVINE      GQFITLFYADRLGYYPHIDEKTGKTVFG---GIPQLGNLKSHLEKAKNDI 97
HYA_BEE         GEEIAILYDP--GMFPALLKDPNGNVVARNGGVPQLGNLTKHLQVFRDHL 95

HYA_BOVINE      AYYIPNDSVG-LAVIDWENWRPTWARNWKPKDVYRDESVELVLQKNPQLS 146
HYA_BEE         INQIPDKSFPGVGVIDFESWRPIFRQNWASLQPYKKLSVEVVRREHPFWD 145

HYA_BOVINE      FPEASKIAKVDFETAGKSFMQETLKLGKLLRPNHLWGYYLFPDCYNHNHN 196
HYA_BEE         DQRVEQEAKRRFEKYGQLFMEETLKAAKRMRPAANWGYYAYPYCYNLTPN 195

HYA_BOVINE      QPTYNGNCPDVEKRRNDDLEWLWKESTALFPSVYLNIRLKSTQNAALYVR 246
HYA_BEE         QP--SAQCEATTMQENDKMSWLFESEDVLLPSVYLRWNLTSGERVGLVG- 242

HYA_BOVINE      NRVQEAIRLSKIASVESPLPVFVYARPVFTDGSSTYLSQGDLVNSVGEIV 296
HYA_BEE         GRVKEALRIARQMTTSRKK-VLPYYWYKYQDRRDTDLSRADLEATLRKIT 291

HYA_BOVINE      SLGASGIIMWGSLNLSLSVQSCMNLGTYLNTTLNPYIINVTLAAKMCSQV 346
HYA_BEE         DLGADGFIIWGSSDDINTKAKCLQFREYLNNELGPAVKRIALNNNANDRL 341

HYA_BOVINE      LCHDGGVCTRKHWNSSDYLHLNPMNFAIQTGEGGKYTVPGTLTLEDLQKF 396
HYA_BEE         TVDVSVDQV---------------------------------------- 350

HYA_BOVINE      SDTFYCSCYSNLSCKKRVDIKNVHSVDVCMAEDVCIDAFLKPP 439
HYA_BEE         -------------------------------------------
```

Figure 1

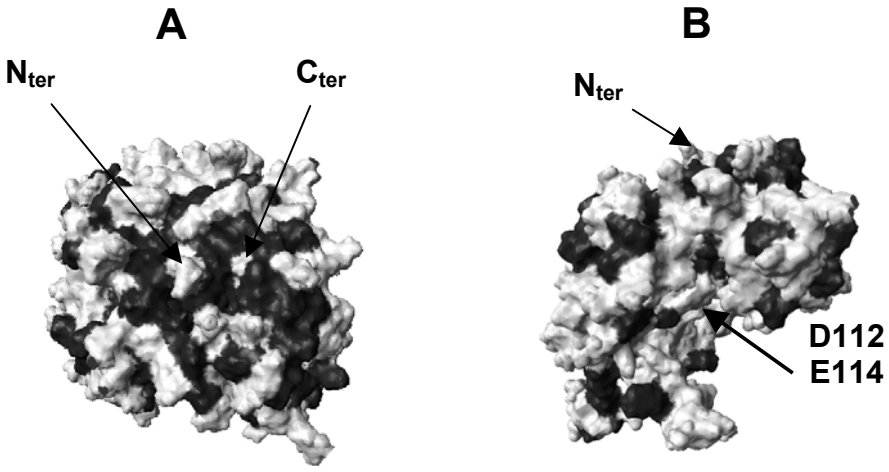

Figure 2

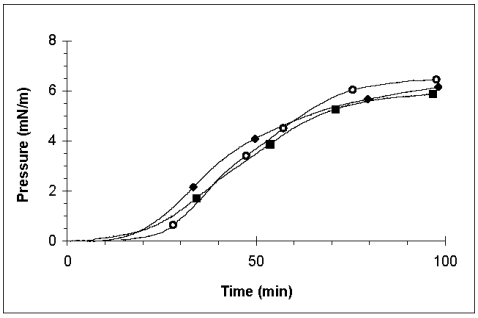

Figure 3

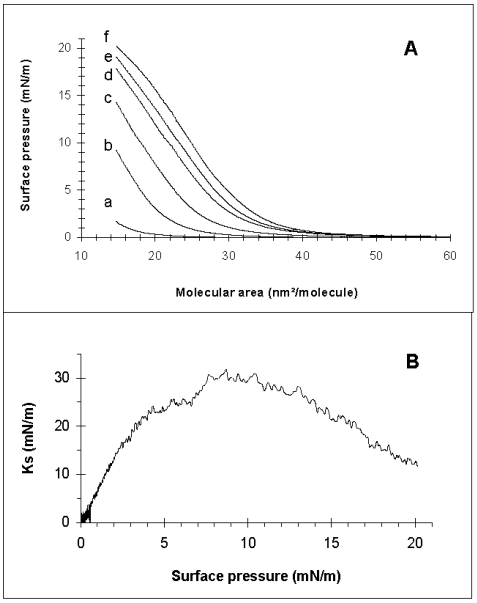

Figure 4

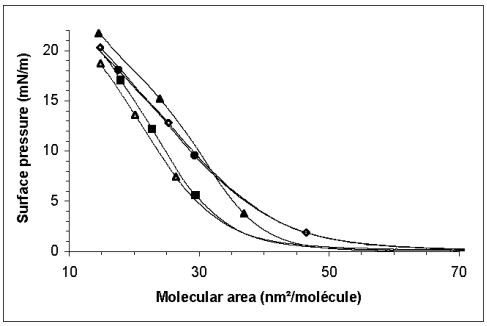

Figure 5

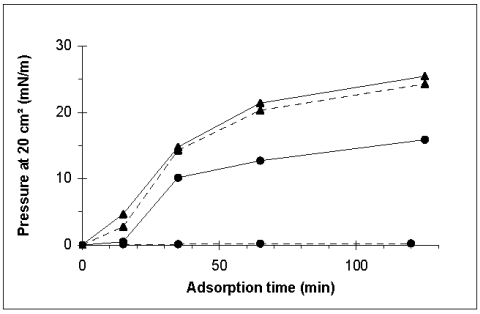

Figure 6

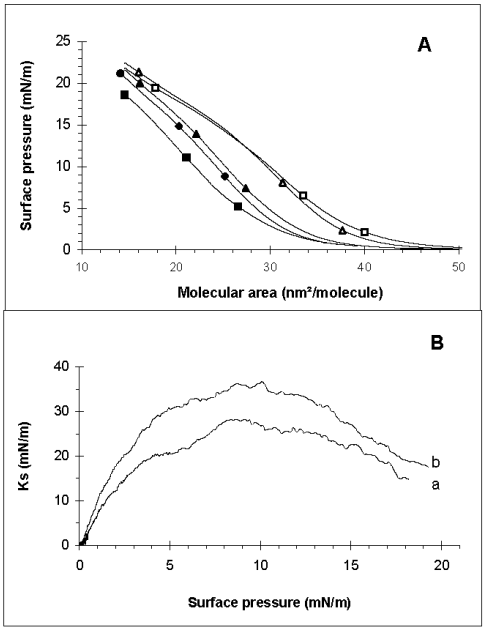

Figure 7

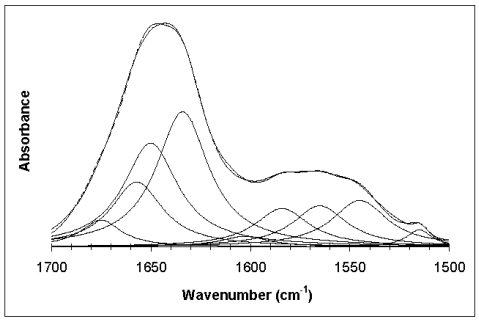

Figure 8

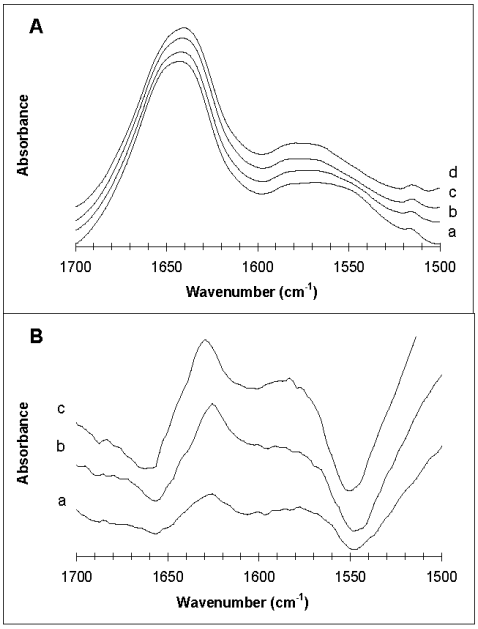

Figure 9